APPLIED ORGANOMETALLIC CHEMISTRY
Appl. Organometal. Chem. 2003; **17**: 421–428
Published online in Wiley InterScience (www.interscience.wiley.com). DOI:10.1002/aoc.449

Synthesis and structures of $[Yb\{\eta^5\text{-}(C_5H_4)B(N^iPr_2)NH^tBu\}_2\{N(SiMe_3)_2\}]$ and $[Zr\{\eta^5\text{-}(C_9H_6)B(N(SiMe_3)_2)(C_9H_7)\}Cl_2]$†

Holger Braunschweig[1]*, Mario Kraft[1], Melanie Homberger[2], Frank M. Breitling[3], Andrew J. P. White[3]‡, Ulli Englert[2]‡ and David J. Williams[3]‡

[1]Institut für Anorganische Chemie, Julius-Maximilians-Universität Würzburg, Am Hubland, D-97074 Würzburg, Germany
[2]Institut für Anorganische Chemie, RWTH Aachen, Professor-Pirlet-Str. 1, D-52056 Aachen, Germany
[3]Department of Chemistry, Imperial College, Exhibition Road, London SW7 2AZ, UK

Received 20 December 2002; Revised 15 January 2003; Accepted 29 January 2003

Both amido-(cyclopentadienyl)boranes and bis(cyclopentadienyl)boranes of the types $R_2NB(C_xH_y)(NR')$ and $R_2NB(C_xH_y)_2$ (R = alkyl, trimethylsilyl; R′ = Ph; $C_xH_y = C_5H_5$ (cyclopentadienyl), C_9H_7 (indenyl), $C_{13}H_9$ (fluorenyl)) were recently shown to form corresponding boron-bridged Group 4 metallocenes that exhibit high activities in Ziegler–Natta-type catalysed olefin polymerization. Here, the same boranes were utilized in the formation of metallocenes of ytterbium and zirconium, where the ligands selectively bind in a non-chelate fashion. The resulting complexes $[Yb\{\eta^5\text{-}(C_5H_4)B(N^iPr_2)NH^tBu\}_2\{N(SiMe_3)_2\}]$ (2) and $[Zr\{\eta^5\text{-}(C_9H_6)B(N(SiMe_3)_2)(C_9H_7)\}Cl_2]$ (4) allow studies on these ligands in a metal-bonded, though unstrained, environment. Furthermore, these complexes might find use as precursors in the formation of organometallic polymers, since they exhibit a readily available moiety for the coordination of further transition metal centres. Both complexes were fully characterized by multinuclear magnetic resonance spectroscopy and X-ray structure determination.

KEYWORDS: boron; boranes; bis(indenyl) ligand; amido(cyclopentadienyl) ligand; ytterbocene; zirconocene

INTRODUCTION

Ansa-metallocenes of Group 4 transition metals represent useful catalysts for the homogeneous Ziegler–Natta-type polymerization of α-olefins, and vivid research on the correlation between the ligand design and the catalytic performance has developed during the last decade.[1–3] In this context, we and others recently published the synthesis of boron bridged ansa-metallocenes **I**[4–11] and corresponding 'constrained geometry' complexes (CGCs) **II**[12] of Group 4 metals (Fig. 1). It was demonstrated that these complexes exhibit an increased catalytic activity due to the Lewis acidity of the threefold coordinated boron[5,13]—though it is cancelled to some extent because of the stabilizing amino group. Furthermore, the high rigidity of the comparably short boron bridge should give rise to a better stereocontrol in the polymerization of propylene and higher α-olefins.

Preparation of the respective ligand precursors is feasible by a convenient multistep one-pot synthesis.[6] Coordination to the transition metal centre is than accomplished by a deprotonation/salt elimination sequence or by amine elimination.[6,12] The reaction sequence is outlined in Fig. 2 for selected examples.

Recently, we reported on the formation of the zirconium complex $[Zr\{\eta^5 : \eta^1\text{-}(C_9H_6)B(N^iPr_2)NPh\}_2]$ (**III**) that contains two chelating boron-bridged constrained-geometry-type ligands bound to the transition metal centre.[14] Although the

*Correspondence to: Holger Braunschweig, Institut für Anorganische Chemie, Julius-Maximilians-Universität Würzburg, Am Hubland, D-97074 Würzburg, Germany.
E-mail: h.braunschweig@mail.uni-wuerzburg.de
†Dedicated to Professor Thomas P. Fehlner on the occasion of his 65th birthday, in recognition of his outstanding contributions to organometallic and inorganic chemistry.
‡X-ray crystallography.
Contract/grant sponsor: BASF AG Ludwigshafen.
Contract/grant sponsor: BMBF.
Contract/grant sponsor: DFG.
Contract/grant sponsor: EPSRC.
Contract/grant sponsor: FCI.
Contract/grant sponsor: Royal Society.

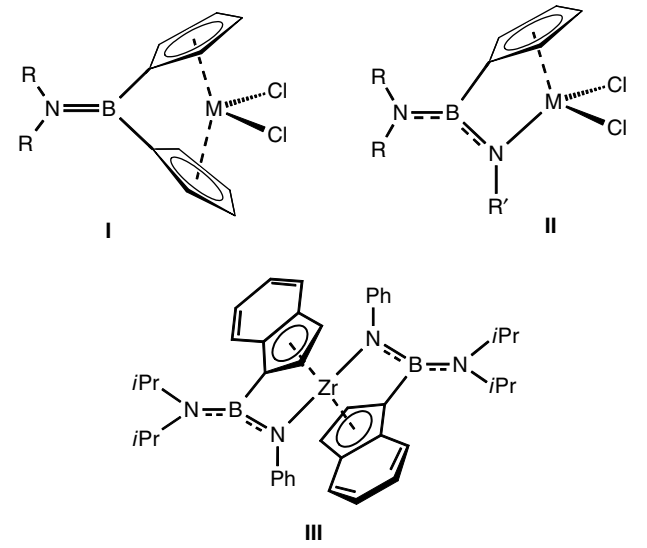

Figure 1. Structures of complexes **I**–**III**.

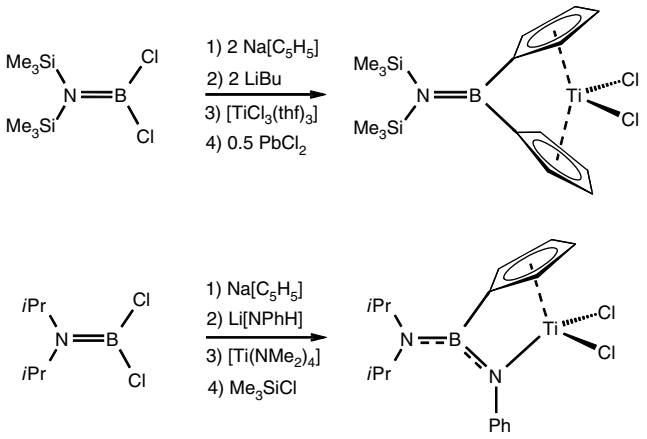

Figure 2. Outline reaction sequence for selected examples.

resulting complex formally has 20 valence electrons, it is best described as an 18-electron metallocene-type complex with additional nitrogen donor groups that contribute, on average, three electrons each.[15]

In the course of our investigations on boron-bridged complexes we synthesized related compounds exhibiting another interesting structural motif, namely complexes containing two of the aforementioned borane ligands in a non-chelating fashion. In the present paper we report on the synthesis of two of these complexes, the ytterbocene [Yb{η^5-(C_5H_4)B(N^iPr_2)NH^tBu}$_2${$N(SiMe_3)_2$}] (**2**) and the zirconocene [Zr{η^5-(C_9H_6)B($N(SiMe_3)_2$)(C_9H_7)}Cl_2] (**4**), by selective monodeprotonation of the ligand precursors and subsequent reaction with the respective transition metal halides. Both complexes are characterized by means of multinuclear magnetic resonance spectroscopy and X-ray diffraction analysis. Apart from being metallocene-type complexes with a sterically very demanding ligand framework, complexes of this type might find use in the formation of organometallic polymers, since they incorporate two additional potential coordination sites.

RESULTS AND DISCUSSION

Ytterbocene complex

Synthetic aspects

Synthesis of the ligand precursor (C_5H_5)B(N^iPr_2)NH^tBu (**1**) was accomplished, following our procedure for the synthesis of boron-bridged CGC-type ligands bearing an NHPh group,[12,14] by subsequent reaction of $^iPr_2NBCl_2$ with Na[C_5H_5] and Li[NH^tBu] (Eqn (1)).

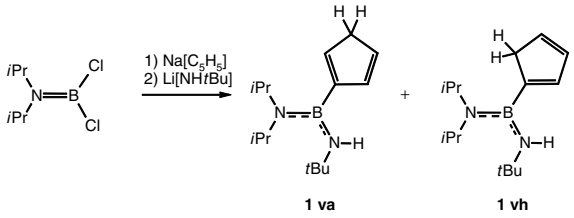

(1)

Intermediate removal of the NaCl formed improves the overall yields slightly. Purification of the crude product by sublimation in high vacuum gives **1** in 79% yield as colourless needles. The ligand precursor is obtained as a 1 : 1 isomeric mixture of vinyl–allyl (**1 va**) and vinyl–homoallyl (**1 vh**) isomers as proven by ^1H and ^{13}C NMR spectroscopy. This observation is in accordance with the levelled formation of **va** and **vh** isomers of the cyclopentadienyl moieties in aminobis(cyclopentadienyl)boranes.[9] Neither isomer can be distinguished in the ^{11}B NMR spectrum, which exhibits a single peak at 29.8 ppm.

The ligand precursor **1** was reacted with two equivalents of the deprotonating agent K[$N(SiMe_3)_2$] at ambient temperature for 2 h, before adding one equivalent of $YbCl_3$ at −78 °C and subsequent stirring at ambient temperature overnight. During this period no apparent colour change could be observed, indicating that no complex formation was accomplished. Only after addition of a small amount of tetrahydrofuran (THF) did the colour change, turning immediately from almost colourless to light red, indicating complex formation. The mixture was then heated to 40 °C for 16 h to allow the reaction to go to completion. The reaction product was obtained in 80% yield (with respect to the ligand precursor) by recrystallization at −30 °C.

X-ray structure determination (*vide infra*) identified the product to be the unbridged metallocene-type complex [Yb{η^5-(C_5H_4)B(N^iPr_2)NH^tBu}$_2${$N(SiMe_3)_2$}] (**2**) instead of the expected CGC [Yb{η^5:η^1-(C_5H_4)B(N^iPr_2)N^tBu}Cl] or a corresponding dimer. Obviously, K[$N(SiMe_3)_2$] is a base weak enough to deprotonate selectively the cyclopentadienyl

moiety only in the boron-bridged CGC-type ligand **1**, since even a comparably long reaction time of 14 h at ambient temperature prior to complex formation did not result in any product with a deprotonated amino moiety. The high yield with respect to the ligand precursor is another indicator for the high selectivity of this reaction. After reaction of two equivalents of the ligand precursor with the $YbCl_3$, the remaining chloride is replaced by $[N(SiMe_3)_2]^-$ due to the excess of $K[N(SiMe_3)_2]$ in the reaction mixture (Fig. 3).

Owing to the paramagnetic nature of **2**, NMR spectroscopic characterization of the compound is not feasible. The ^1H NMR spectrum at ambient temperature shows only two very broad peaks, at −23 and 77 ppm, whereas the ^1H NMR spectrum at −60 °C exhibits nine broad signals between −45 and 130 ppm, which cannot be attributed based on either chemical shifts or integral ratios. Apparently, the paramagnetic ytterbium centre strongly affects the relaxation of protons, which are quite remote, i.e. more than three bonds apart. A similar observation was reported for $[Yb(\eta^5\text{-}C_5H_5)_2(OR)_2]$ (R = alkyl) complexes.[16] Nevertheless, ^{11}B NMR spectroscopy seems to be a useful tool to monitor the progress of complex formation, since the product shows a signal at 8.7 ppm that is high field shifted by about 21 ppm with respect to the corresponding signal in the free ligand. In comparison, coordination of similar CGC-type ligands to diamagnetic titanium or zirconium moieties causes only moderate high field shifts, so that signals for starting material and product are usually not resolved (compare also the ^{11}B NMR chemical shifts for bis(indenyl)borane **3** and zirconocene **4** (*vide infra*)).[6,7] On the other hand, comparably distinct shifts of ^{11}B NMR signals were reported for the ytterbium complex $[\{\eta^5\text{:}\eta^1\text{-}(C_9H_6)B(N^iPr_2)(C_2B_{10}H_{10})\}Yb][Li(dme)_3]$.[17]

Structural characterization

In the crystal, molecules of **2** show crystallographic C_2 symmetry (Fig. 4) with ytterbium and N(1) on a twofold axis. The cyclopentadienyl ligands of the bent metallocene structure subtend a dihedral angle of 48.54(14)°. Distances between ytterbium and the cyclopentadienyl carbon atoms range from 2.553(3) Å for Yb–C(3) to 2.679(2) Å for Yb–C(1), with a resulting ring slippage between the projection of the metal atom on the ring and the centre of gravity of 0.13 Å away from the substituted atom C(1). Both the arrangement of N(1) and the two cyclopentadienyl centres of gravity around the metal and the coordination around N(1) (Si, Si′, Yb) are planar for reasons of symmetry. Both borane ligands show very similar geometry; therefore, only the arrangement in the

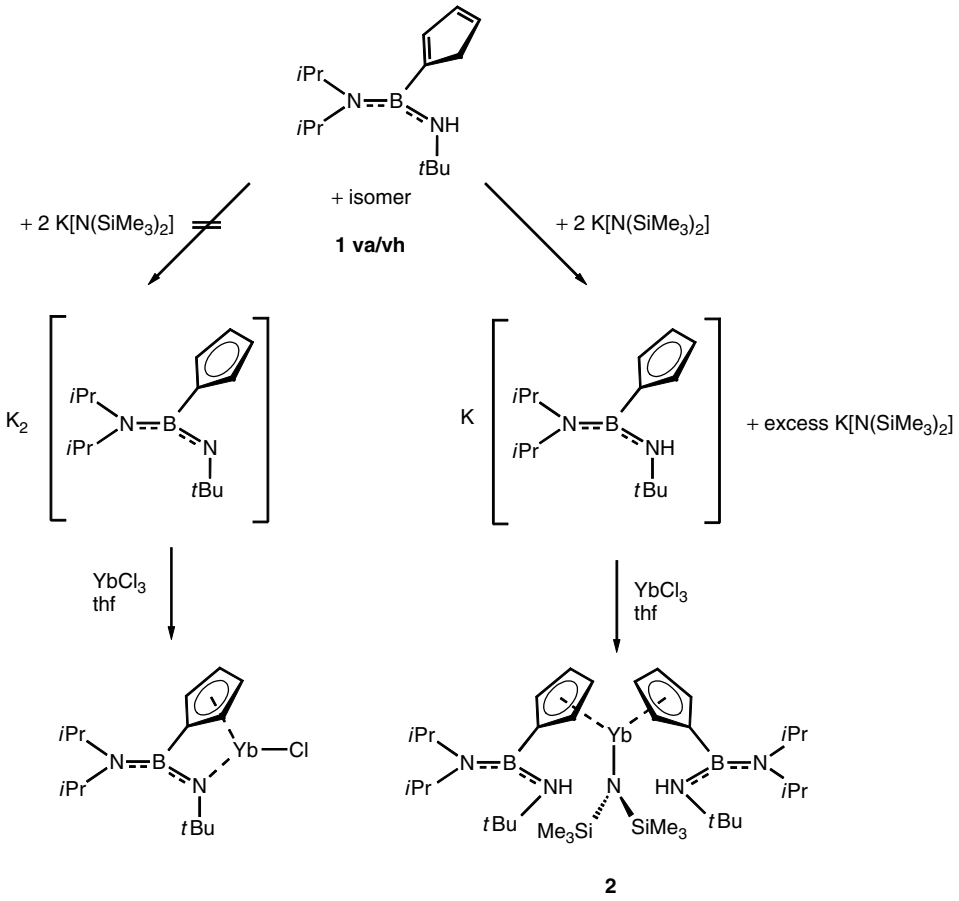

Figure 3. Reaction sequence for **2** from **1 va**/**vh**.

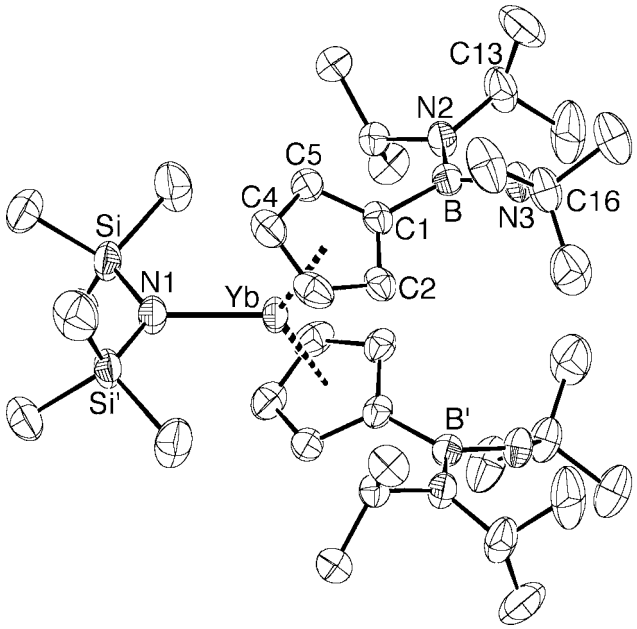

Figure 4. Structure of **2** in the crystal.

B(1)-based ligand is discussed. No significant deviation from planarity is found for the boron coordination. It involves a relatively long C(1)–B(1) distance of 1.587(4) Å and two B–N separations of almost equal length, namely B(1)–N(2) 1.432(2) and B(1)–N(3) 1.427(3) Å. The shortest intermolecular interactions in the solid state are due to H···H contacts of *ca* 2.4 Å between neighbouring molecules. Other selected bonding parameters for **2** are listed in Table 1.

Zirconocene complex

Synthetic aspects

Synthesis of the ligand precursor $(Me_3Si)_2NB(C_9H_7)_2$ (**3**) and formation of the corresponding [1]borazirconocenophane $[Zr\{(\eta^5\text{-}C_9H_6)_2BN(SiMe_3)_2\}Cl_2]$ have been previously reported.[7] Here, we describe the preparation of the corresponding zirconocene $[Zr\{\eta^5\text{-}(C_9H_6)B(N(SiMe_3)_2)(C_9H_7)\}Cl_2]$ (**4**), in which each ligand coordinates in a non-chelate fashion with only one of its indenyl substitutents to the transition metal centre. Complex **4** was obtained in moderate yield by a two-step sequence involving the selective monodeprotonation of the ligand precursor with one equivalent of butyl lithium and subsequent salt elimination reaction with $[ZrCl_4(thf)_2]$ (Eqn (2)).

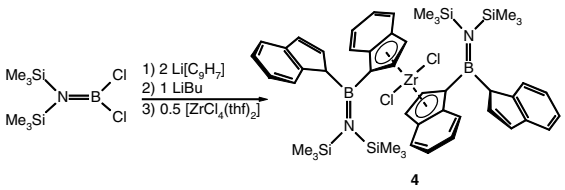

(2)

Apparently, the ligand precursor is preferably mono deprotonated in the presence of only one equivalent of butyl lithium, rather than being statistically deprotonated at both indenyl moieties. This is most probably due to the higher charge density of the dianionic species. The moderate yield, though, indicates that a certain amount of double deprotonation might occur as a side reaction.

The structure of **4** in solution was derived from multinuclear magnetic resonance spectra. The ^1H NMR spectrum shows a wide complex aromatic area between 5.4 and 7.8 ppm, a signal at 3.52 ppm for the protons at the saturated carbon atoms in the indenyl rings that are not coordinated to the zirconium centre, and resolved peaks at 0.30 and 0.31 ppm for the two sets of chemically non-equivalent trimethyl silyl groups. The ^{11}B NMR exhibits a signal at 54.7 ppm that is only slightly high field shifted with respect to the ^{11}B NMR signal of the free ligand, therefore impeding monitoring of the reaction progress by means of ^{11}B NMR spectroscopy.

As previously reported, the ligand precursor is initially obtained as the kinetically controlled product, i.e. both indenyl moieties are attached with the saturated carbon atom to boron.[7] Isomerization via sigmatropic rearrangement is possible at higher temperatures or in the presence of catalytic amounts of amines (Eqn (3)).[7,9,14,18–22]

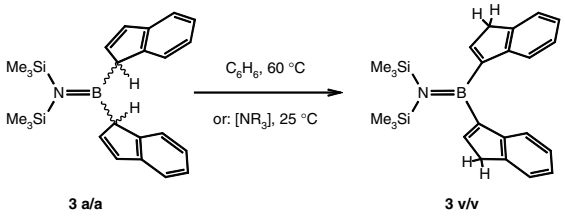

(3)

The protons at the saturated carbon atoms in the indenyl moieties are significantly different in the ^1H NMR spectrum for the two respective isomers, with 3.61 ppm for the kinetically controlled product and 3.22 ppm for the thermodynamically more stable rearranged isomer.[7] In the ^1H NMR spectrum of complex **4**, the chemical shift and integral value of the peak at 3.52 ppm indicate that the non-coordinating indenyl moieties of the ligands are still bound to the boron centres via their saturated carbon atom. This demonstrates that no

Table 1. Selected bond lengths (Å) and angles (°) for **2**

Yb–N(1)	2.206(3)	N(3)–B	1.426(3)
Si–N(1)	1.701(14)	C(1)–C(2)	1.415(3)
N(2)–B	1.432(3)	C(1)–B	1.587(3)
X(1)–Yb–X(2)	48.54(14)	N(3)–B–N(2)	117.7(2)
Si–N(1)–Si′	123.66(16)	N(3)–B–C(1)	119.5(2)
Si–N(1)–Yb	118.17(8)	N(2)–B–C(1)	122.81(19)
Si′–N(1)–Yb	118.17(8)		

rearrangement occurs under the reaction conditions and that no lithium–proton exchange occurs between protonated and deprotonated indenyl fragments.

The constitution of the compound could be confirmed in the solid state by X-ray structure determination. Suitable single crystals of **4** for X-ray analysis were obtained by recrystallization from CH_2Cl_2 at −35 °C.

Structural characterization

A single crystal X-ray analysis showed the structure of ligand **3** (which has been reported previously, but to a noticeably lower precision[7]) to have approximate C_2 symmetry about an axis collinear with the B(1)–N(1) bond (Fig. 5). The boron and nitrogen centres both possess trigonal planar geometries, being only 0.009 Å and 0.022 Å respectively out of the planes of their substituents, with in each case the sum of the angles around the central atom being within 0.1° of 360°. The two trigonal planes are, however, very markedly twisted with respect to each other (by *ca* 51°), and this, combined with the relatively long B(1)–N(1) distance of 1.422(3) Å, precludes any significant interaction with the non-bonding nitrogen p-orbital. The two indenyl ring systems are nearly flat, the maximum deviations from planarity in each case being less than 0.017 Å, and there is only a slight folding (*ca* 5°) of the B–C bonds out of their respective indenyl planes. The planes of the C_5 rings are noticeably rotated with respect to the BNC_2 plane (each by *ca* 41°), so there seems little likelihood of any substantial interaction between the C=C double bond and the 'unused' p-orbital on the boron centre. Within the C_5-ring portion of the C(1)/C(9) indenyl ring system there is some clear bond localization: the C(1)–C(5), C(2)–C(3) and C(3)–C(4) bonds are single in nature (Table 2), whereas the C(1)–C(2) linkage [1.343(4) Å] is evidently a formal double bond; the aromatic character of the C(4)–C(5) bond [1.404(3) Å] is equally clear. (An equivalent pattern of bonding is seen in the C(11)/C(19) ring system.) Adjacent molecules are held together by a pair of weak intermolecular C–H···π interactions between (i) C(17)–H and the C(14) to C(19) ring, and (ii) C(19)–H and the C(4) to C(9) ring (with H···π (Å) and C–H···π (°) of (i) 2.92, 140 respectively and (ii) 3.00, 147 respectively) to form loosely linked chains that propagate along the crystallographic *b* direction.

Table 2. Selected bond lengths (Å) and angles (°) for **3**

B(1)–N(1)	1.442(3)	B(1)–C(11)	1.565(3)
B(1)–C(1)	1.576(3)	N(1)–Si(20)	1.758(2)
N(1)–Si(24)	1.766(2)	C(1)–C(2)	1.343(4)
C(1)–C(5)	1.484(3)	C(2)–C(3)	1.505(3)
C(3)–C(4)	1.501(4)	C(4)–C(5)	1.404(3)
C(11)–C(12)	1.344(4)	C(11)–C(15)	1.488(3)
C(12)–C(13)	1.500(4)	C(13)–C(14)	1.496(4)
N(1)–B(1)–C(11)	120.3(2)	N(1)–B(1)–C(1)	120.3(2)
C(11)–B(1)–C(1)	119.3(2)	B(1)–N(1)–Si(20)	118.4(2)
B(1)–N(1)–Si(24)	118.1(2)	Si(20)–N(1)–Si(24)	123.43(11)

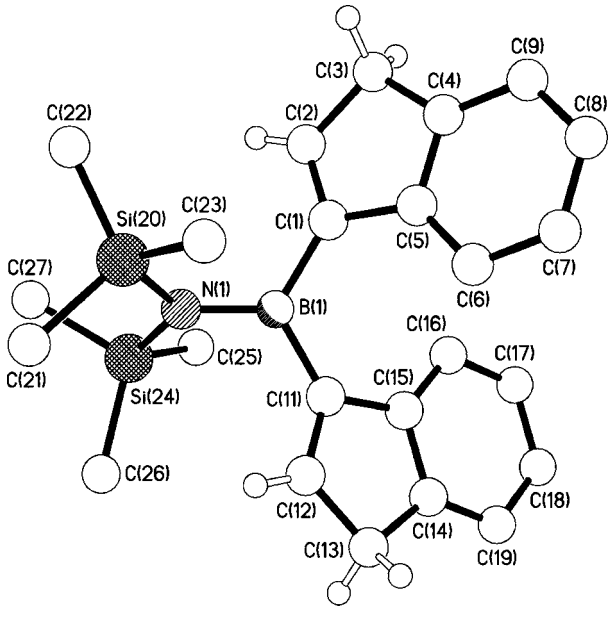

Figure 5. Structure of **3** in the crystal.

A structural determination on crystals of **4** revealed the formation of the zirconium bis(diindenyl) complex shown in Fig. 6. As was observed in the structure of the related ligand precursor **3**, the complex has molecular (but not crystallographic) C_2 symmetry, here about an axis bisecting the Cl(1)–Zr–Cl(2) angle. Considering the interaction between the metal centre and the C_5-ring portion of each indenyl ring system as a sole 'bond' to the centroid of each C_5 ring [X(1) and X(2) for the C(1)/C(5) and C(31)/C(35) ring systems respectively], then the geometry at zirconium is distorted tetrahedral with angles in the range 90.95(3) to 130.8(1)°, the most acute and obtuse being for the Cl(1)–Zr–Cl(2) and X(1)–Zr–X(2) angles respectively (Table 3). (The associated Zr–X separations are 2.246(3) Å and 2.245(3) Å to X(1) and X(2) respectively.) The two coordinated indenyl ring systems are disposed in a pseudo eclipsed fashion, but rotated such that the two C_6 rings are oriented one 'position' out of register, the C(4)/C(9) ring sitting 'above' Cl(2) and the C(34)/C(39) ring sitting 'below' Cl(1) (Fig. 6).

In general, the two bis(indenyl)borane ligands have similar geometries and so, in the interests of simplicity, the discussion will focus on the B(1)-based ligand with, unless stated otherwise, equivalent parameters for the B(2) ligand given in square brackets. As was the case in **3**, the boron and nitrogen centres here are both trigonal planar, the central atoms being 0.072 Å [0.060 Å] and 0.083 Å [0.089 Å] out of the planes of their substituents respectively (the sums of the angles around the two centres are within 0.7° [0.9°] of 360°) and the two trigonal planes are rotated with respect to each other by *ca* 45° [44°] (*cf.* 51° in **3**). The boron–nitrogen bond length of 1.442(5) Å [1.434(5) Å] is not statistically different

Table 3. Selected bond lengths (Å) and angles (°) for **4**

Zr–X(1)	2.246(3)	Zr–X(2)	2.245(3)
B(1)–N(1)	1.442(5)	N(1)–Si(24)	1.767(3)
N(1)–Si(20)	1.770(3)	B(2)–N(2)	1.434(5)
N(2)–Si(50)	1.769(3)	N(2)–Si(54)	1.775(3)
Cl(1)–Zr–X(1)	105.7(1)	X(1)–Zr–X(2)	130.8(1)
Cl(1)–Zr–X(2)	108.9(1)	Cl(2)–Zr–X(2)	105.3(1)
N(1)–B(1)–C(1)	120.7(3)	Cl(2)–Zr–X(1)	108.0(1)
C(1)–B(1)–C(11)	120.4(3)	N(2)–B(2)–C(41)	118.1(3)
N(2)–B(2)–C(31)	121.5(3)	B(2)–N(2)–Si(50)	121.8(2)
C(31)–B(2)–C(41)	120.0(3)	Si(50)–N(2)–Si(54)	118.1(2)

from that seen in **3** and, combined with the substantial twist described above, again indicates an absence of any significant contribution from the nitrogen non-bonding p-orbital.

Unlike **3**, within each bis(indenyl)borane ligand here the two indenyl ring systems are distinctly different, most noticeably in that for the C(11)/C(19) and C(41)/C(49) ring systems the carbon linked to the boron atom is protonated (i.e. sp^3 hybridized), whereas for the C(1)/C(9) and C(31)/C(39) ring systems it is not (sp^2 hybridized). This has an associated marked effect on the B(1)–C distances, with that to the metal-coordinated indenyl ring system, B(1)–C(1) 1.570(5) Å [1.573(5) Å], being noticeably shorter than that to its non-coordinated counterpart, B(1)–C(11) 1.608(5) Å [1.613(5) Å]. In contrast to **3**, where the B–C bonds were nearly coplanar with their associated C_5 rings, here the bonds are noticeably out of plane, with bends of *ca* 12° [10°] and 61° [56°] to the coordinated and non-coordinated ring systems respectively. The non-equivalence of the two indenyl ring systems is also evidenced by their tilt angles with respect to the BNC_2 plane, being *ca* 34° [34°] and 84° [74°] for the C_5-ring portions of the coordinated and non-coordinated indenyl ring systems respectively. Though the greater tilting correlates with the noticeably longer B–C bond length (*vide supra* and *cf.* **3**) these observations are probably independent consequences of sp^3 *cf.* sp^2 hybridization rather than being directly linked to each other. The coordinated indenyl rings are markedly distorted: C(1), C(2), C(3) and C(5) are planar to within 0.003 Å, with C(4) 0.074 Å out of this plane; C(4)/C(9) has a boat-like distortion such that C(4), C(6), C(7) and C(9) are coplanar to within 0.009 Å, with C(5) and C(8) 0.073 Å and 0.026 Å respectively out of this latter plane. The C(31)/C(39) indenyl ring has a different distortion: C(31), C(32), C(33) and C(35) are coplanar to within 0.004 Å, with C(34) 0.073 Å out of this plane; the C(34)/C(39) ring has a twisted conformation where C(36), C(37), C(38) and C(39) are coplanar to within 0.014 Å, with C(34) and C(35) +0.036 Å and −0.033 Å respectively out of this plane on opposite sides.

The different hybridizations for the boron-bound carbon atom of the coordinated and non-coordinated indenyl rings within each bis(indenyl)borane ligand have a consequent marked effect upon the pattern of bonding within the respective C_5 rings. The arrangements seen for the non-coordinated ring systems C(11)/C(15) and C(41)/C(45) are very similar to those observed in **3**, but with the boron atom bound to the other side of the C_5 ring (in **3** the boron was linked to the double bond carbon atom adjacent to the six-membered ring, whereas here it is bound to the methylene carbon). Within the coordinated rings, however, the bonding is more delocalized, with four of the five distances in the range 1.405(5) to 1.424(5) Å [1.415(5) to 1.432(5) Å], the fifth (between C(1) and C(5) [C(31) and C(35)]) being noticeably longer at 1.448(5) Å [1.450(5) Å].

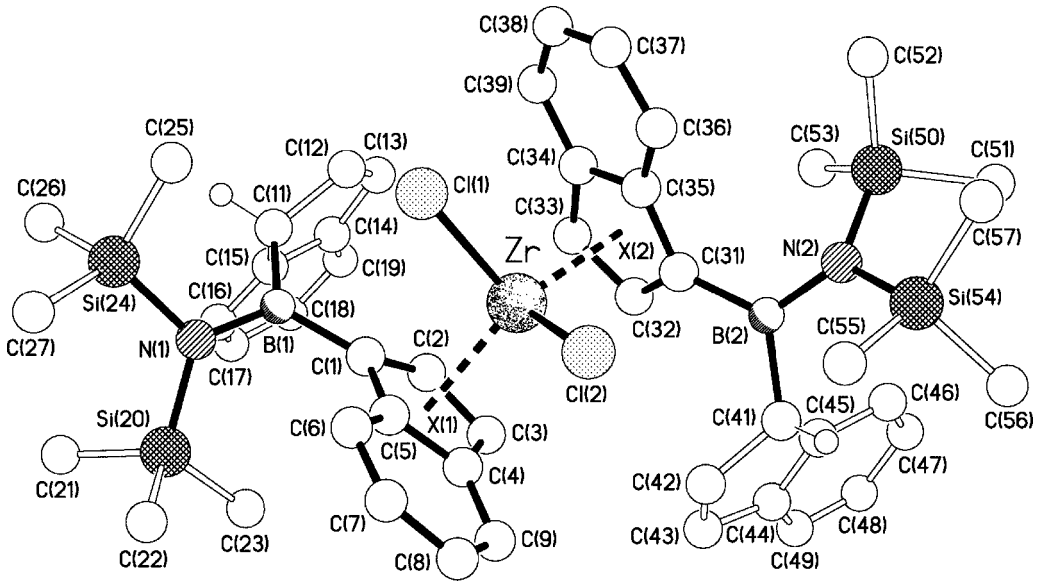

Figure 6. Structure of **4** in the crystal.

The molecules pack to form discrete centrosymmetric dimers held together by pairs of intermolecular edge-to-face C–H···π interactions between the C(19)–H proton on one C_6 aromatic ring and the centroid of the C(34)/C(39) C_6 aromatic ring, with an H···π distance of 3.14 Å and a C–H···π angle of 156°; the centroid···centroid separation is 5.37 Å and the two rings are inclined by *ca* 88°.

EXPERIMENTAL

Syntheses

All manipulations were carried out under a dry nitrogen atmosphere with common Schlenk techniques. Solvents and reagents were dried by standard procedures, distilled, and stored under nitrogen over molecular sieves. $^{i}Pr_2NBCl_2$,[23] $(Me_3Si)NBCl_2$,[24] $Na[C_5H_5]$, and $Li[C_9H_7]$[25] were obtained according to literature procedures, whereas $Li[NH^tBu]$ was obtained by stochiometric addition of BuLi to a solution of *tert*-butyl amine in hexane. NMR: Varian Unity 500 at 499.843 MHz (^{1}H, external standard tetramethylsilane (TMS)), 150.364 MHz (^{11}B, $BF_3{\cdot}OEt_2$ in C_6D_6 as external standard), 125.639 MHz ($^{13}C\{^1H\}$, APT, internal standard TMS); JEOL JNM-EX270 at 270.166 MHz (^{1}H, external standard TMS), 86.680 MHz (^{11}B, $BF_3{\cdot}OEt_2$ in C_6D_6 as external standard). Mass spectra were recorded on a Finnigan MAT 95 (70 eV).

*$C_5H_5B(N^iPr_2)NH^tBu$ (**1 va/vh**)*

$Na[C_5H_5]$ (3.97 g, 45.1 mmol) was suspended in 50 ml hexane and a solution of $^{i}Pr_2NBCl_2$ (8.19 g, 45.1 mmol) in 50 ml hexane was added dropwise at 0 °C. The resulting suspension was allowed to come to ambient temperature and stirred for 16 h. The precipitated NaCl was filtered off and washed with 20 ml hexane. The filtrate was than added dropwise to a suspension of $Li[NH^tBu]$ (3.56 g, 45.1 mmol) in 30 ml hexane/10 ml diethyl ether at 0 °C. The slightly yellow mixture was stirred for 16 h at ambient temperature. After removing the precipitated NaCl by filtration and evaporating the solvent, sublimation at 70 °C under high vacuum yielded an isomer mixture of **1 va/vh** as colourless crystals (8.83 g, 79%).

^{1}H NMR (benzene-d_6): $\delta = 1.08$, 1.12 (2d, 12H, Me^{i}_{Pr}); 1.15, 1.18 (2s, 9H, Me^{t}_{Bu}); 2.86, 3.05 (2m, 2H, CH_2); 3.24, 3.37 (2m, 1H, CH^{i}_{Pr}); 6.40–6.76 (m, 3H, CH_{Cp}). ^{13}C NMR (benzene-d_6): $\delta = 23.26$, 23.34 (br, Me^{i}_{Pr}); 33.69, 33.86 (Me^{t}_{Bu}); 43.06 (CH_2); 45.68, 45.99 (CH^{i}_{Pr}); 46.85 (CH_2); 49.28, 49.37 (Me_3C); 131.78, 133.51, 133.81, 135.35, 135.43, 137.92 (CH_{Cp}). ^{11}B NMR (CD_2Cl_2): $\delta = 29.8$. MS; m/z (%): 248 (9) [M^+], 233 (46) [$M^+ - Me$], 191 (8) [$M^+ - {}^tBu$], 148 (4) [$M^+ - {}^tBu - {}^iPr$].

*$[Yb\{\eta^5\text{-}(C_5H_4)B(N^iPr_2)NH^tBu\}_2\{N(SiMe_3)_2\}]$ (**2**)*

1 va/vh (1.67 g, 6.76 mmol) was dissolved in 20 ml toluene and a solution of $K[N(SiMe_3)_2]$ in 40 ml toluene was added at ambient temperature. The resulting suspension was stirred for a further 2 h, then cooled to −78 °C. $YbCl_3$ (1.61 g, 5.78 mmol) was added and the mixture was allowed to come to ambient temperature. After stirring for another 12 h, 2 ml THF was added, resulting in an immediate colour change of the suspension to light red. The mixture was heated to 40 °C for 16 h to ensure completion of the reaction. The insoluble fraction was removed by filtration. Concentrating the remaining solution and storing at −30 °C yielded **4** as red crystals (2.24 g, 80% with respect to **1 va/vh**).

^{11}B NMR (CD_2Cl_2): $\delta = 8.7$. MS; m/z (%): 666 (1) [$M^+ - N(SiMe_3)_2$], 581 (100) [$M^+ - C_5H_4B(N^iPr_2)NH^tBu$], 482 (11) [$M^+ - C_5H_4B(N^iPr_2)NH^tBu - N^iPr_2$], 320 (5) [$\{Yb(\eta^5\text{-}C_5H_4BNH^tBu\}$], 247 (5) [$C_5H_4B(N^iPr_2)NH^tBu$], 146 (54) [$N(SiMe_3)SiMe_2$].

*$[Zr\{\eta^5\text{-}(C_9H_6)B(N(SiMe_3)_2)(C_9H_7)\}Cl_2]$ (**4**)*

$Li[C_9H_7]$ (2.44 g, 20.0 mmol) was suspended in 40 ml toluene and a solution of $[(Me_3Si)_2NBCl_2]$ (2.41 g, 10.0 mmol) in 10 ml toluene was added dropwise at 0 °C. The mixture was allowed to come to ambient temperature and stirred for 16 h. LiCl was filtered off, the remaining clear yellowish solution was cooled to 0 °C and LiBu (6.25 ml, 10.0 mmol) was added slowly. The solution was stirred for 16 h at ambient temperatures, then cooled to −78 °C and $[ZrCl_4(thf)_2]$ (1.89 g, 5.00 mmol) was added at once. The mixture was allowed to warm up slowly and, after getting to room temperature, stirred for further 2 h. The precipitate formed was removed by filtration, the solution concentrated and upon cooling to −35 °C yielded **4** as orange microcrystals (1.16 g, 24%). Recrystallization from CH_2Cl_2 gave orange crystals suitable for X-ray structure determination.

^{1}H NMR (benzene-d_6): $\delta = 0.30$ (s, 18H, Me_3Si); 0.31 (s, 18H, Me_3Si); 3.52 (s, 2H, BCH); 5.4–7.8 (m, 24H, C_9H_6/C_9H_7). ^{11}B NMR (benzene-d_6): $\delta = 54.7$.

X-ray structure determination

*Crystal structure of compound **2** ($C_{36}H_{74}B_2N_5Si_2Yb$)*

$C_{36}H_{74}B_2N_5Si_2Yb$, $M = 827.8$, monoclinic, $C2/c$ (no. 15), $a = 20.808(5)$, $b = 13.1910(15)$, $c = 18.972(3)$ Å, $\beta = 122.390(13)°$, $V = 4397.2(14)$ Å^3, $Z = 4$, $D_c = 1.25$ g cm^{-3}, μ(Mo Kα) = 2.21 mm^{-1}, $T = 213$ K, irregular fragment of a large red block; 4792 absorption-corrected independent reflections, F^2 refinement, $R_1 = 0.024$, $wR_2 = 0.057$, 4234 independent observed reflections [$|F_o| > 4\sigma(|F_o|)$, $2\theta = 54°$], 219 parameters. CCDC 201564.

*Crystal structure of compound **3** ($C_{24}H_{32}BNSi_2$)*

$C_{24}H_{32}BNSi_2$, $M = 401.5$, monoclinic, $I2/a$ (no. 15), $a = 23.716(2)$, $b = 7.025(1)$, $c = 29.570(3)$ Å, $\beta = 103.62(1)°$, $V = 4788.0(8)$ Å^3, $Z = 8$, $D_c = 1.114$ g cm^{-3}, μ(Mo Kα) = 0.16 mm^{-1}, $T = 203$ K, pale yellow prismatic blocks; 4226 independent measured reflections, F^2 refinement, $R_1 = 0.048$, $wR_2 = 0.111$, 3082 independent observed reflections [$|F_o| > 4\sigma(|F_o|)$, $2\theta = 50°$], 253 parameters. CCDC 201460.

Crystal structure of compound **4** *($C_{48}H_{62}B_2N_2Si_4Cl_2Zr{\cdot}3CH_2Cl_2$)*

$C_{48}H_{62}B_2N_2Si_4Cl_2Zr{\cdot}3CH_2Cl_2$, $M = 1217.9$, triclinic, $P\bar{1}$ (no. 2), $a = 11.309(1)$, $b = 16.554(1)$, $c = 17.077(2)$ Å, $\alpha = 97.15(1)$, $\beta = 107.22(1)$, $\gamma = 95.52(1)^\circ$, $V = 3000.0(5)$ Å^3, $Z = 2$, $D_c = 1.348$ g cm^{-3}, μ(Cu Kα) $= 5.81$ mm^{-1}, $T = 203$ K, orange blocks; 8908 independent measured reflections, F^2 refinement, $R_1 = 0.044$, $wR_2 = 0.115$, 7970 independent observed absorption corrected reflections [$|F_o| > 4\sigma(|F_o|)$, $2\theta = 120^\circ$], 658 parameters. CCDC 201461.

SUPPLEMENTARY MATERIAL

Crystallographic data (excluding structure factors) for the structures reported in this paper have been deposited with the Cambridge Crystallographic Data Centre as supplementary publication nos CCDC 201564 (**2**), CCDC 201460 (**3**) and CCDC 201461 (**4**). Copies of the data can be obtained free of charge on application to CCDC, 12 Union Road, Cambridge CB2 1EZ, UK [fax: +44-1223-336-033; e-mail: deposit@ccdc.cam.ac.uk].

Acknowledgements

This work was supported by BASF AG Ludwigshafen, BMBF, DFG, EPSRC, FCI, RSoc. F.M.B. thanks FCI for a pre-doctoral scholarship.

REFERENCES

1. Brintzinger HH, Fischer D, Mülhaupt R, Rieger B, Waymouth RM. *Angew. Chem.* 1995; **107**: 1255; *Angew. Chem. Int. Ed. Engl.* 1995; **34**: 1143 and references cited therein.
2. Kaminski W. *J. Chem. Soc. Dalton Trans.* 1998; 1413 and references cited therein.
3. Gladysz JA (ed.). *Chem. Rev.* 2000; **100**(4): and references cited therein.
4. Braunschweig H, Dirk R, Müller M, Nguyen P, Gates DP, Manners I. *Angew. Chem.* 1997; **109**: 2433; *Angew. Chem. Int. Ed. Engl.* 1997; **36**: 2338.
5. Braunschweig H, von Koblinski C, Kristen MO. Patent O.Z. 0050/49643, 1998; submitted.
6. Braunschweig H, von Koblinski C, Wang R. *Eur. J. Inorg. Chem.* 1999; 69.
7. Braunschweig H, von Koblinski C, Mamuti M, Englert U, Wang R. *Eur. J. Inorg. Chem.* 1999; 1899.
8. Berenbaum A, Braunschweig H, Dirk R, Englert U, Green JC, Lough AJ, Manners I. *J. Am. Chem. Soc.* 2000; **122**: 5765.
9. Braunschweig H, von Koblinski C, Neugebauer M, Englert U, Zheng X. *J. Organometal. Chem.* 2001; **619**: 305.
10. Ashe AJ, Fang X, Kampf JW. *Organometallics* 1999; **18**: 2288.
11. Shapiro PJ. *Eur. J. Inorg. Chem.* 2001; 321 and references cited therein.
12. Braunschweig H, von Koblinski C, Englert U. *Chem. Commun.* 2000; 1049.
13. Klang JA, Collum DB. *Organometallics* 1988; **7**: 1532.
14. Braunschweig H, von Koblinski C, Breitling FM, Radacki K, Hu C, Wesemann L, Marx T, Pantenburg I. *Inorg. Chim. Acta* 2002; in press.
15. Okuda J, Amor F, du Plooy KE, Eberle T, Hultzsch KC, Spaniol TP. *Polyhedron* 1998; **17**: 1073.
16. Steudel A, Siebel E, Fischer RD, Paolucci G, Lucchini V. *J. Organometal. Chem.* 1998; **556**: 229.
17. Zi G, Li HW, Xie Z. *Organometallics* 2002; **21**: 1136.
18. Mikhailov BM, Baryshnikova TK, Bogdanov VS. *Zh. Obsch. Khim.* 1973; **43**: 1949.
19. Herberich GE, Barday E, Fischer A. *J. Organometal. Chem.* 1998; **567**: 127.
20. Gridnev ID, Meller A. *Main Group Met. Chem.* 1998; **21**: 271.
21. Knizek J, Krossing I, Nöth H, Ponikwar W. *Eur. J. Inorg. Chem.* 1998; 505.
22. Barday E, Frange B, Hanquet B, Herberich GE. *J. Organometal. Chem.* 1999; **572**: 225.
23. Gerrard W, Hudson HR, Mooney EF. *J. Chem. Soc.* 1960; 5168.
24. Geymayer P, Rochow EG, Wannegat U. *Angew. Chem.* 1964; **76**: 499.
25. Brandsma L. *Preparative Organometallic Chemistry*, vol. 2. Springer: Berlin, 1990; 45.

